

AD-A072 101

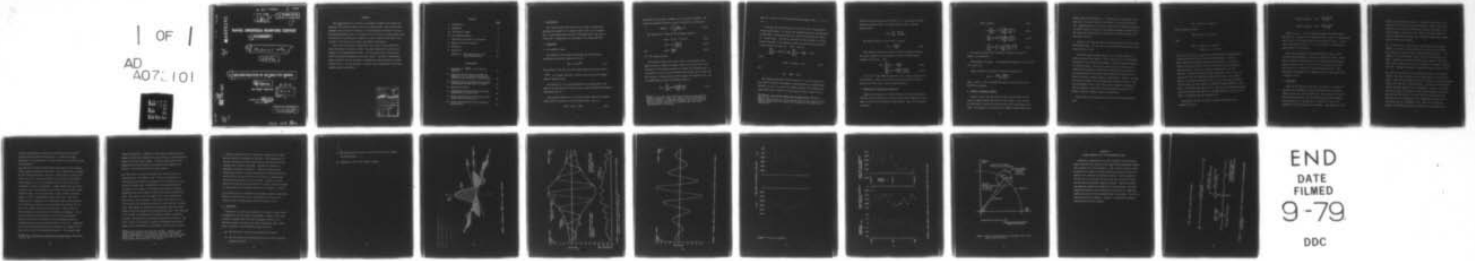
NAVAL UNDERSEA WARFARE CENTER SAN DIEGO CA
RECONSTRUCTION OF AN ANALYTIC SIGNAL.(U)
NOV 67 L P MULCAHY
NUWC-TN-38

F/6 9/3

UNCLASSIFIED

NL

| OF |
AD
A072 101



END
DATE
FILMED
9-79
DDC

MOST Project-3

00U1B1

LEVEL

14

NUWC-TN-38

001838

MA072101

NAVAL UNDERSEA WARFARE CENTER

11 November 1967

9 Technical note

12 24p.

Dood
FG

6 RECONSTRUCTION OF AN ANALYTIC SIGNAL.

10 L.P. Mulcahy

San Diego, California

DDC
RECEIVED
JUL 30 1979
A

SUBPROJECT 16 F1710316
TASK NO. 8685

DISTRIBUTION STATEMENT A

Approved for public release
Distribution Unlimited

DDC FILE COPY

001838

SP-13

403 023 Gen

FOREWORD

This note describes the results of an attempt to compute the envelope and frequency of an analytic signal from a set of sampled data. This note has been prepared since it may be of interest to a limited number of persons at the U. S. Navy Undersea Warfare Center. It should not be construed as a formal report since its function is to present for information a small portion of work which is applicable to the area of sonar signal measurements and analysis.

This note was written as a term paper for a course in signal analysis at Purdue University in the Fall of 1966. The paper presented the results of an analysis of an interferogram waveform. It was assumed at that time that the reader had intimate acquaintance with such a device. Therefore, the method of signal generation was not discussed. In making this paper available as a NUWC Technical note, it is now necessary to include a short description of the interferogram signal in Appendix A.

Accession For	
NTIS GR&I	<input checked="" type="checkbox"/>
DDC TAB	<input type="checkbox"/>
Unannounced	<input type="checkbox"/>
Justification	<input type="checkbox"/>
<i>ditto in file</i>	
By _____	
Distribution/ _____	
Availability Codes	
Dist.	Avail and/or special
A	

CONTENTS

	<u>Page</u>
1. Introduction	1
2. Background	1
2.1 The Analytic Signal	1
2.2 The Sampling Theorem	2
3. Computation of Envelope and Frequency	4
4. Results of Computer Analysis	5
5. Discussion	8
6. Conclusions	12
Appendix A: Short Description of the Interferogram Signal	20

ILLUSTRATIONS

1. Comparison of $\frac{\text{Sin}(t)}{t}$ and its Hilbert transform	14
2. Comparison of the computed envelope and frequency with the computed interferogram waveform in the region of the central peak	15
3. Computed Hilbert transform of the computed interferogram waveform shown in Figure 2	16
4. Overlay for Figure 5	17
5. Interferogram reconstruction for data far removed from the central peak	18
6. Phasor representation of the analytic form of the sum of two sine waves	19
A-1 General characteristics of the interfero- gram waveform	21

1. Introduction.

This report presents the results of an attempt to compute the envelope and frequency of an analytic signal from a set of sampled data. Interferogram data from run 4 (flashlight bulb) were used as a data base. Computations were performed on the Purdue IBM 7094.

2. Background.

2.1 The analytic signal.

The definition of envelope and frequency may be obtained by considering the analytic signal of the form

$$\tilde{f}(t) = V(t) e^{j\phi(t)} \quad (2-1)$$

The envelope is then the real time varying function $V(t)$ where $V(t) > 0$.

$e^{j\phi(t)}$ is a complex function, a phasor, which rotates with angular (radian) frequency $\dot{\phi}(t)$.

The question is, if we are presented with an analog signal, $f(t)$, which is a real function of time, how can we obtain envelope and frequency information from it?

The procedure used here is to consider another form of the analytic signal which is equivalent to the one given above. That is,

$$\tilde{f}(t) = f(t) + j \hat{f}(t) \quad (2-2)$$

where $\hat{f}(t)$ is the Hilbert transform of $f(t)$ (written as $H\{f(t)\}$ and called the quadrature function of $f(t)$) and $H\{f(t)\}$ is defined as*

$$H\{f(t)\} = \frac{1}{\pi} \int_{-\infty}^{\infty} \frac{f(\tau)}{(t-\tau)} d\tau \quad (2-3)$$

The equivalence is shown by the following relations:

$$V(t) = \{f^2(t) + \hat{f}^2(t)\}^{1/2} \quad (2-4)$$

$$\phi(t) = \tan^{-1} \left\{ \frac{\hat{f}(t)}{f(t)} \right\} \quad (2-5)$$

and
$$\dot{\phi}(t) = \frac{d\phi(t)}{dt} \quad (2-6)$$

2.2 The sampling theorem

The sampling theorem states that, given a time function, $f(t)$, which contains no frequencies higher than W Hz, and also given a set of samples of the function spaced no more than $1/2 W$ seconds apart, it is possible to recover the intervening values of the time function with full accuracy. Reconstruction of the original time function, $f(t)$, can be accomplished by using the following relation:

$$f(t) = \sum_{n=-\infty}^{\infty} f(n\Delta t) \frac{\sin(\pi \frac{t}{\Delta t} - n\pi)}{(\pi \frac{t}{\Delta t} - n\pi)} \quad (2-7)$$

*One has to be careful when referring to some texts for tables of Hilbert transforms. There are a number of ways of defining the Hilbert transform, all depending on whether one wants to end up with the original function or its negative after two Hilbert transformations in succession.

where $\Delta t = 1/2 W$ is the time interval between samples and $n = \dots -1, 0, +1, \dots$.

To see why this relation works, we will first look at the spectrum of the sampled signal. In effect, the sampling process may be considered as equivalent to multiplying $f(t)$ by a train of delta-functions spaced Δt seconds apart. The Fourier transform of such a product is a train of delta-functions in the frequency domain convolved with the spectrum of the original time function $f(t)^*$. That is,

$$\sum_{n=-\infty}^{\infty} \delta(t - n\Delta t) f(t) \iff \sum_{m=-\infty}^{\infty} \delta(\omega + m \frac{2\pi}{\Delta t}) * F(\omega)$$

where

$$f(n\Delta t) = f(t) \delta(t - n\Delta t) \quad (2-8)$$

and

$$f(t) \iff F(\omega).$$

The frequency spectrum of $f(n\Delta t)$ consists of a train of replicas of $F(\omega)$ spaced at positive and negative integer multiples of $2\pi/\Delta t$ radians. Therefore, in order to recover the original spectrum (and assuming spectrum overlap between adjacent spectrum replicas doesn't occur)** it is

*A. Papoulis, The Fourier Integral and its Application, McGraw-Hill, 1962, p. 48.

**This is the equivalent to the restriction given in the statement of the sampling theorem where the samples must be spaced no more than $1/2 W$ seconds apart.

sufficient to pass the spectrum centered at $\omega = 0$ and reject all other replicas by using an ideal rectangular band pass filter with the characteristics

$$H(\omega) = \begin{cases} 1 & |\omega| < B \\ 0 & \text{elsewhere.} \end{cases}$$

The impulse response of this filter is simply

$$I(t) = \frac{\sin Bt}{Bt} \quad (2-9)$$

Thus, when the time function $f(n\Delta t)$ is passed through the filter the output waveform is the convolution of $f(n\Delta t)$ with the impulse response of the filter. Then

$$f(t) = \sum_{n=-\infty}^{\infty} f(n\Delta t) * \frac{\sin Bt}{Bt} \quad (2-10)$$

$$= \sum_{n=-\infty}^{\infty} f(n\Delta t) \frac{\sin B(t - n/2\omega)}{B(t - n/2\omega)} \quad (2-11)$$

If we set $B = 2\pi\omega = \pi/\Delta t$ then equation (2-11) becomes equation (2-7). The relation $B = 2\pi\omega$ is a convenient one since this point is midway between the center of $F(\omega)$ and its adjacent replica.

3. Computation of envelope and frequency.

Equation (2-7) gives us a relation between $f(t)$ (the reconstructed function) and the sampled values of $f(t)$ (the original function), $f(n\Delta t)$. What we now need is the quadrature function $\hat{f}(t)$. This can be obtained as follows:

$$\hat{f}(t) = H\{f(t)\} \quad (3-1)$$

$$= H \left\{ \sum_{m=-\infty}^{\infty} f(n\Delta t) \frac{\sin(\pi \frac{t}{\Delta t} - m\pi)}{(\pi \frac{t}{\Delta t} - m\pi)} \right\} \quad (3-2)$$

$$= \sum_{m=-\infty}^{\infty} f(n\Delta t) H \left\{ \frac{\sin(\pi \frac{t}{\Delta t} - m\pi)}{(\pi \frac{t}{\Delta t} - m\pi)} \right\} \quad (3-3)$$

$$= \sum_{m=-\infty}^{\infty} f(n\Delta t) \left[\frac{1 - \cos(\pi \frac{t}{\Delta t} - m\pi)}{(\pi \frac{t}{\Delta t} - m\pi)} \right] \quad (3-4)$$

The $\sin(x)/x$ function and its Hilbert transform are shown in Figure 1 for comparison.

The envelope and phase are computed using equations (2-4), (2-5), (2-7), and (3-4).

Radian frequency is computed by using the approximation

$$\dot{\phi}(t_i) = \frac{\phi(t_i) - \phi(t_{i-1})}{t_i - t_{i-1}}$$

where t_i and t_{i-1} are two neighboring points in time for which $f(t)$ and $\hat{f}(t)$ are computed.

4. Results of computer analysis.

Figures 2 and 3 show the results of the reconstruction over the interval (sample number) 393 seconds to 435 seconds. This interval was sufficient to enclose the central peak of the interferogram waveform. All waveforms in the figures were computed using original data

samples numbered 375 through 455. In other words, in equations (2-11) and (3-4) n was varied from 375 to 455 while t was varied from 393 to 435. Rough indications are that the accuracy of the computed amplitudes is within 2% and the accuracy of the computed frequency is within 1% of the values that would result if n varied over a much wider range (say for $n < 355$ and $n > 475$).

Figures 4 and 5 show the results of reconstruction over the interval 230 to 250 seconds. In this case n was varied from 200 to 640 and t was varied from 230 to 250.

The interferogram waveform appears to have remained negative in value over most of the interval. This is due to the 12 Hz noise which was added to the interferometer waveform. Also the computed frequency is a peculiar shape. Note that the positive peaks in frequency are rounded and correspond to the greatest (most negative) excursions of the time function or the greatest (most positive) excursions of its Hilbert transform, whichever happens to predominate. Whereas, the negative peaks are sharper and more jagged than the positive peaks. They also correspond in time to the lesser (least negative) excursions of the time function or the lesser (least positive) excursions of its Hilbert transform, whichever happens to predominate.

These effects can be explained if we consider the following waveform:

$$f(t) = A_1 \cos \omega_1 t + A_2 \cos \omega_2 t$$

and its Hilbert transform

$$\hat{f}(t) = A_1 \sin \omega_1 t + A_2 \sin \omega_2 t$$

then

$$\begin{aligned} \tilde{f}(t) = & A_1 \{ \cos \omega_1 t + j \sin \omega_1 t \} \\ & + A_2 \{ \cos \omega_2 t + j \sin \omega_2 t \} \end{aligned}$$

If we set $A_1 \gg A_2$ and $\omega_1 \ll \omega_2$ we have a situation which corresponds quite closely with that existing with the interferogram data. Figure 6 shows a phasor representation for the above equations. We see that maximum velocity of a point on the tip of the phasor representing $\tilde{f}(t)$ takes place when A_1 and A_2 are colinear and pointing in the same direction. Conversely, minimum velocity takes place when A_1 and A_2 are colinear but this time pointing in opposite directions. This minimum velocity can actually be negative if $A_1 \omega_1 > A_2 \omega_2$. The maximum (minimum) velocity takes place when $|f(t)|$ is a maximum (minimum) and $\hat{f}(t)$ is zero when A_1 is pointing along the real axis. Conversely the maximum (minimum) velocity takes place when $|\hat{f}(t)|$ is a maximum (minimum) and $f(t)$ is zero when A_1 is pointing along the imaginary axis.

From Figure 6 we can see that the maximum and minimum for the frequency of $f(t)$ is

$$\text{maximum frequency: } \dot{\phi}(t) = \frac{A_1 \omega_1 + A_2 \omega_2}{A_1 + A_2}$$

$$\text{minimum frequency: } \dot{\phi}(t) = \frac{A_1 \omega_1 - A_2 \omega_2}{A_1 - A_2}$$

Since $A_1, A_2, \omega_1, \omega_2 > 0$ the maximum frequency will always remain well behaved. However, for the minimum frequency, when A_1 is approximately equal to $(A_2 - \epsilon)$ the denominator becomes arbitrarily small. (ϵ is a small number greater than 0). If $\omega_1 < \omega_2$ we observe a large negative-going "spike" in the frequency.

The overall appearance of the waveform $\tilde{f}(t)$ is that of a coil rotating counterclockwise at a rate of ω_1 radians per second. At the tip of the phasor describing this coil is another phasor tracing out another smaller coil at a faster rate of $\omega_2 \gg \omega_1$ radians per second. This coil too is rotating in a counterclockwise direction. This description also appears to be appropriate for the interferogram data in Figures 4 and 5.

5. Discussion.

Until now the subject treated here was primarily an outline of a technique for computing the envelope and frequency of an analytic signal as based on a set of sampled data, and an exposure to some of the experimental results that can be obtained using the technique. Hardly touched on was the subject of exceptions to some of the hypotheses used for generating the technique. Also glossed over was

mention of errors and their sources. And last but not least is the question of the utility of the analytic signal. What we shall do at this point is to list some of the above subjects especially as they can be related to the data at hand. What we will end up with is a series of questions with partial and incomplete answers which suggest areas for future investigation.

5.1 Of what utility is the analytic signal computation technique? Perhaps it is best to talk about analytic waveforms only for narrow-band signals, and then only when a specific application exists. For example, it is not known what utility exists for interferogram waveforms. Examples can be drawn from other areas, however. Sonar and radar returns (echoes) many times have components of doppler associated with them. Perhaps this method of computing frequency would be useful.

5.2 What are the exceptions to the hypotheses used for the sampling theorem? The primary exception is the requirement for a band limited signal. Band limited signals do not exist in nature. In general, physical signals exist only over a finite interval. The spectra of such signals contain frequency components at all frequencies. However, a spectrum may contain energy concentrated at some central frequency so as to be approximately band limited. In such a case the energy outside the band limits may be "negligible" or the signal may be filtered to cut this energy down to a negligible level. There still remains the problem of estimating the amount of variation in the computation of

envelope and frequency of such data as a function of the amount of spectrum falling outside the band limits. In other words, how negligible is a good question. How much accuracy do we sacrifice using this assumption?

5.3 What are the effects of data acquisition devices on the accuracy of the computed envelope and frequency? This is impossible to estimate for the interferogram data. But we can at least point out some of the sources of error. Finite quantization levels, finite width aperture of the sampler, jitter in the sampling time, and circuit noise all contribute to errors in measurement. Lumped together the total effect is equal to that of an equivalent noise source in series with an ideal noiseless signal. We also assume that an ideal infinite resolution sampler is used for measuring the signal plus noise. Thus, when reconstruction is attempted, the reconstructed value of the functions $f(t)$ and $\hat{f}(t)$ will each have errors contributed to them from all the time series samples used in the reconstruction. These errors are carried through in the computation of envelope and frequency. We can say that those time series samples closest to the reconstructed functions in time will contribute not only the greatest amount to reconstruction, but also the greatest amount to the error. Indications are that the reconstructed value of the functions are subject to the same errors as each of the sampled data points.* This subject needs

*R. Bracewell, The Fourier Transform and its Applications, McGraw-Hill, 1965, p. 203.

further investigation. Regardless of the amount of added noise the computed envelope and frequency will appear to have a smooth appearance. Figures 4 and 5 are good examples. The quantization levels of the sampled data are quite evident on the graph of the computed time function. Yet the reconstruction is quite smooth.

5.4 What effect do finite data samples have on the accuracy of reconstruction? The problem is this. Say we are interested in reconstructing the envelope and frequency of a waveform over a time interval T seconds long. Contributions to the reconstruction of the function at any point in time within that interval is made by neighboring time series samples on both sides of the reconstruction point. The closer in time the samples are to the reconstruction point the more they contribute to the value of the function.* Let us now bracket the reconstruction point by a time interval T' seconds long. Then suppose we perform the reconstruction using time series samples within $\pm T'/2$ seconds of the reconstruction point. How large must T' be in order to reconstruct $f(t)$ and $\hat{f}(t)$ to within a specified accuracy? Two reasons for answering this question can be given. The first is that if our accuracy is going to be degraded some certain amount due to the effects of the equivalent noise discussed in part

*This is true in general for both $f(t)$ and $\hat{f}(t)$. However, if the reconstruction point is the same point in time as a time series sample, contributions to $f(t)$ come only from that time series sample and no other. Whereas, contributions to $\hat{f}(t)$ come from all time series samples except that one. See Figure 1.

5. There is not much point in carrying out computations to a much greater accuracy by including too much data. Also computations of the sort necessary for reconstruction take an appreciable amount of computer time, and time costs money. Therefore it would be an advantage to be able to estimate T' . Section 4 discussed some results where the most accurate reconstruction of the functions $f(t)$ and $\hat{f}(t)$ within the interval 395 to 435 seconds was obtained from data within the interval 355 to 475 seconds. Looking at the end points of the smaller interval we find T' is equal to about 40 seconds (or data points since the points were set at one sample per second).

5.5 How much error is introduced by the digital computer computations?

We have no idea how much error is introduced but we can point to round-off error as being possibly the chief source of error.

6. Conclusions

Computation of envelope and frequency of an analytic signal based on sampled data has been shown to be feasible. However, there exist a number of problem areas that need investigation before we can specify the amount of accuracy that these computations yield. These areas constitute a list of possible sources of error:

- a. The error due to the use of non-band limited signals,
- b. The error caused by the equivalent noise associated with data acquisition devices. *→ next page*

c. The approximation error due to the use of finite data samples
in reconstruction. *and*

d. Computation error in the digital computer.

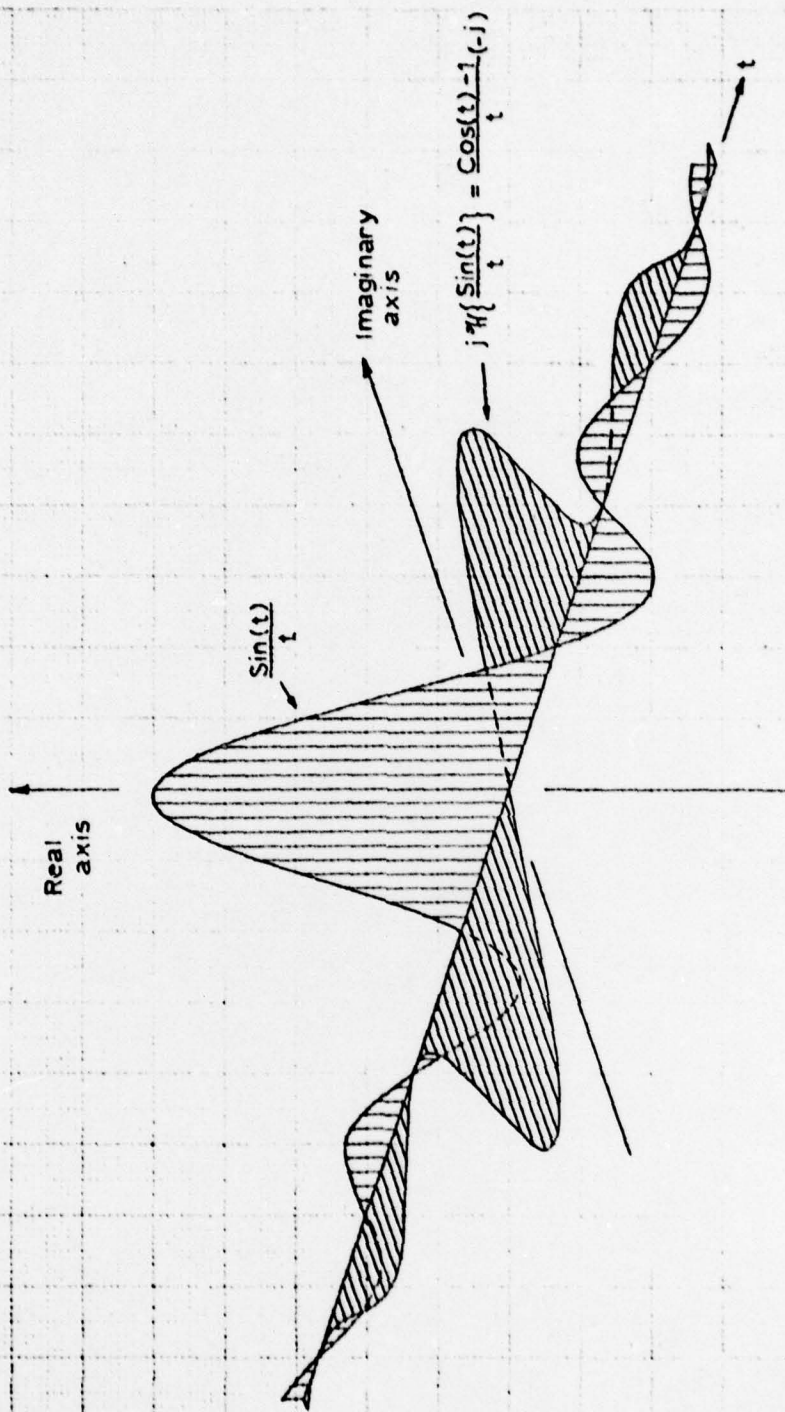


FIGURE 1. Comparison of $\frac{\sin(t)}{t}$ and its Hilbert transform.

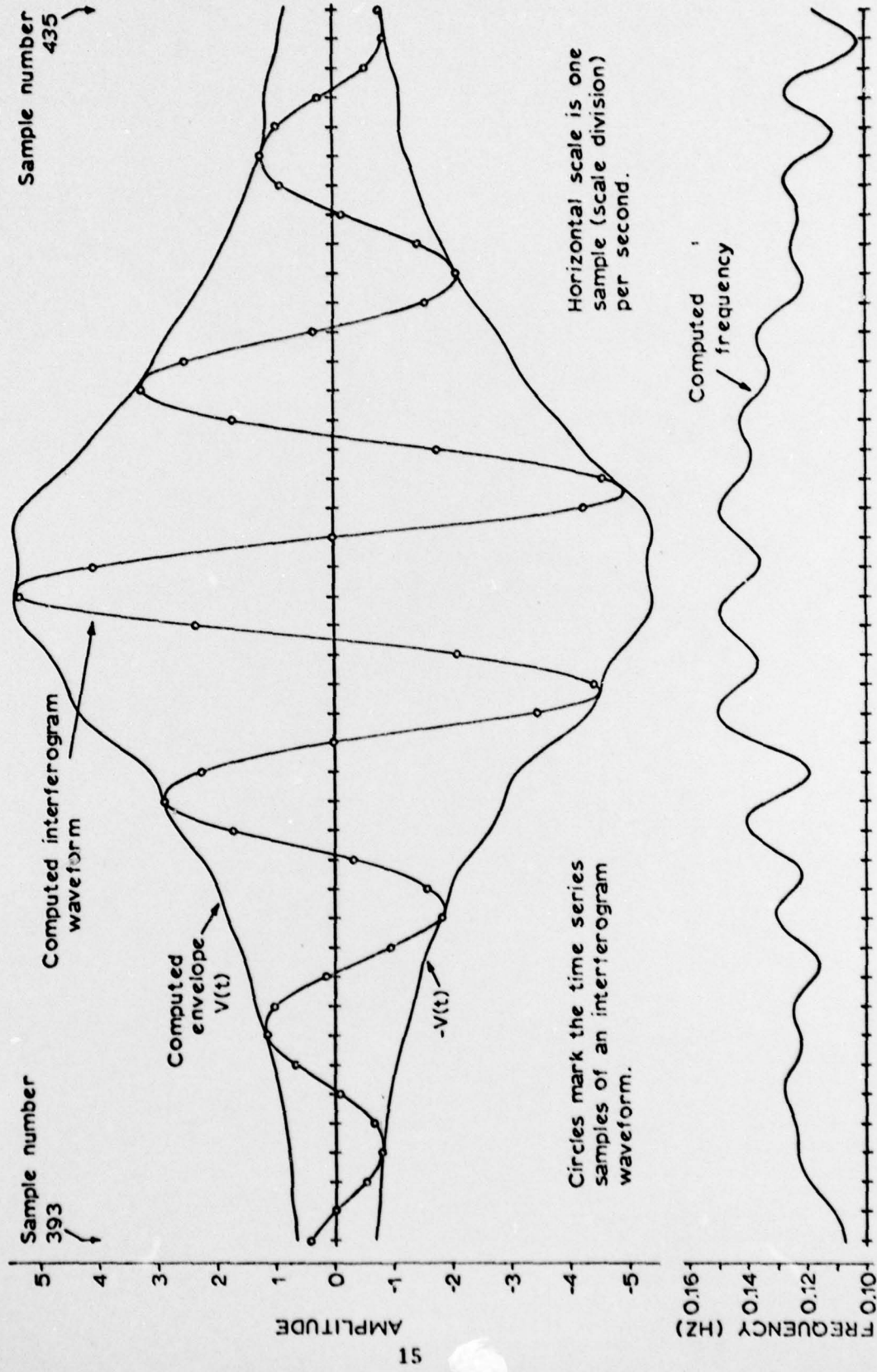


FIGURE 2. Comparison of the computed envelope and frequency with the computed interferogram waveform in the region of the central peak.

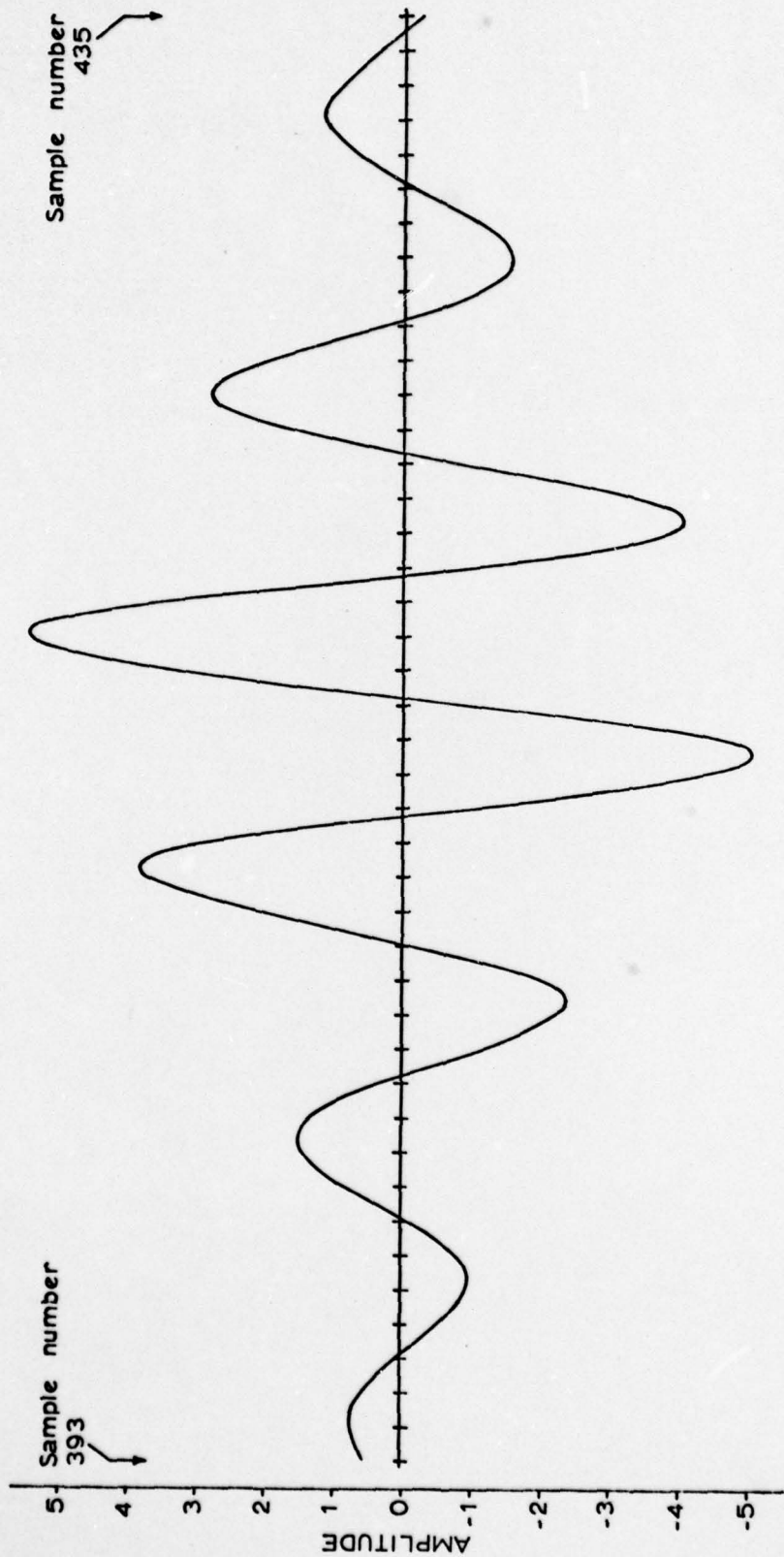


FIGURE 3. Computed Hilbert transform of the computed interferogram waveform shown in Figure 2.

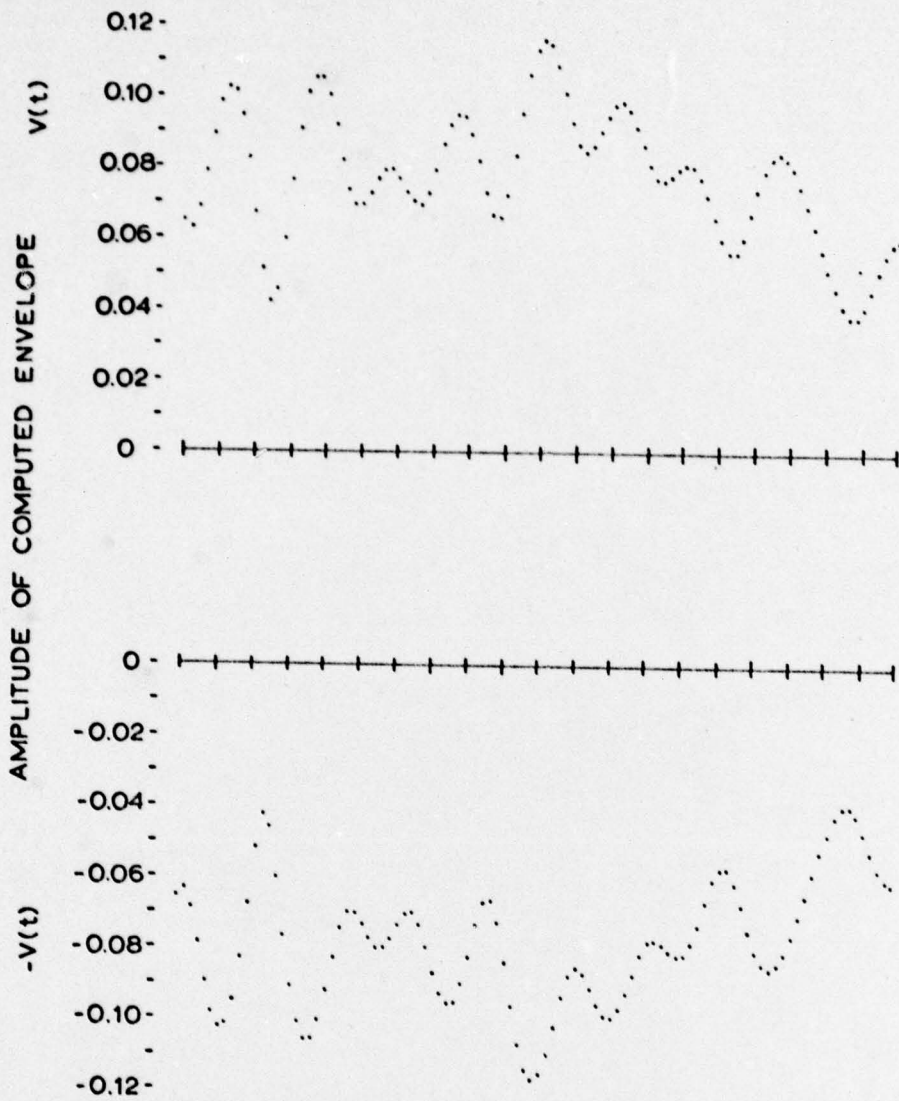


FIGURE 4. Overlay for Figure 5.

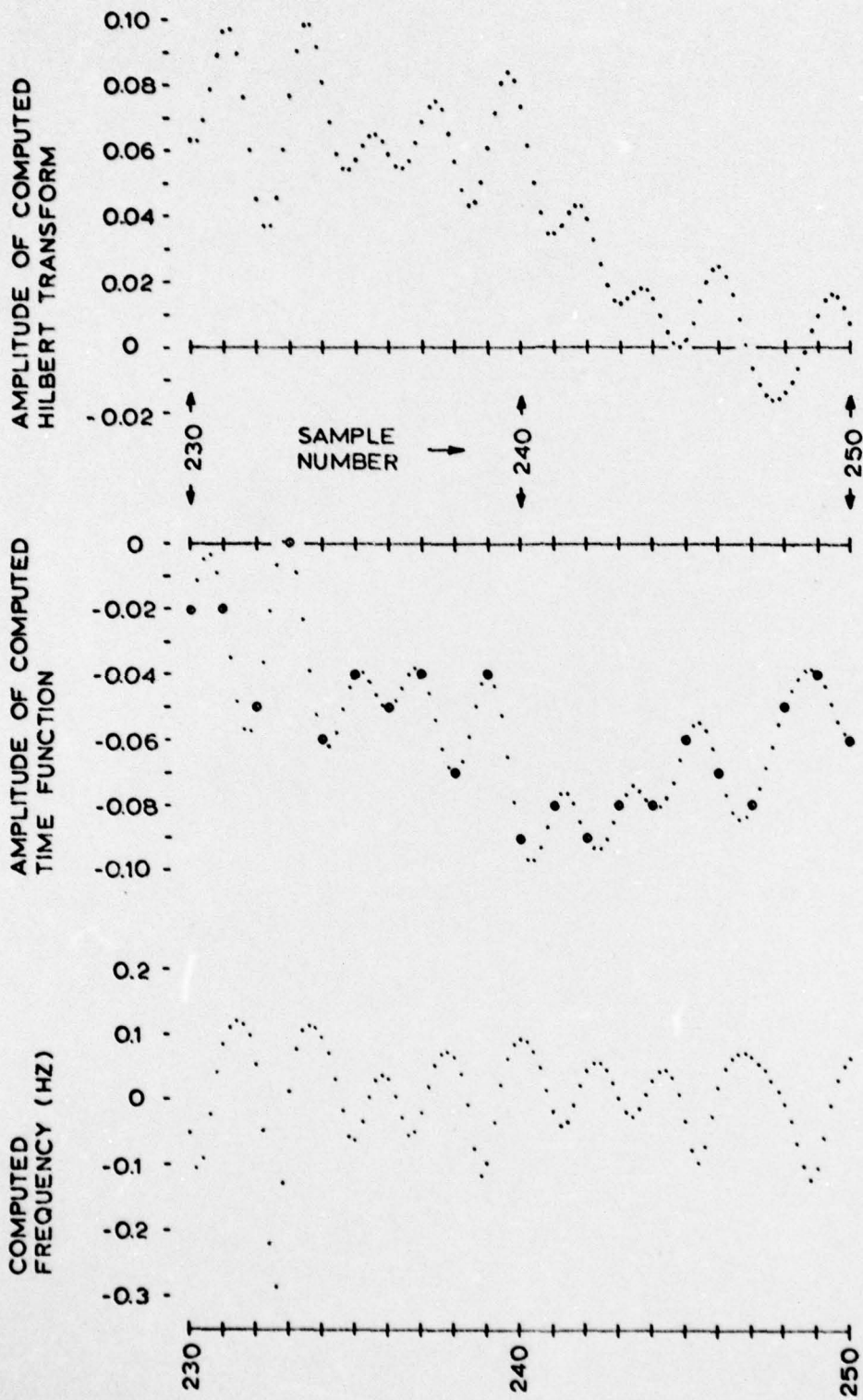
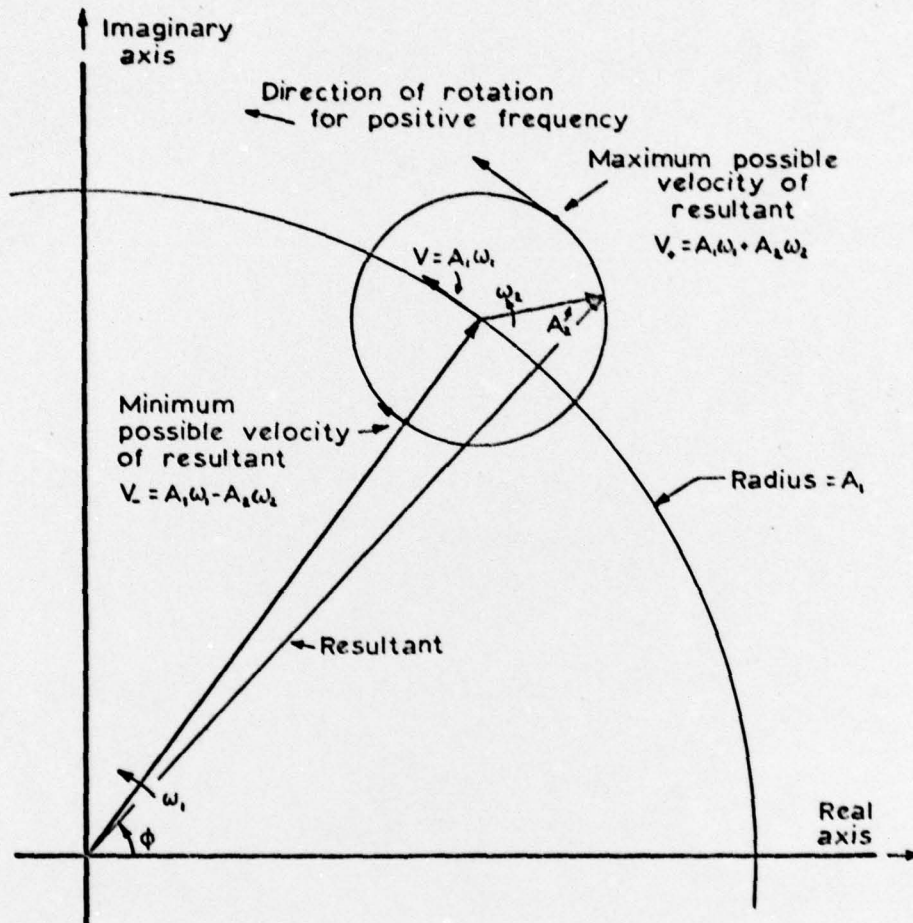


FIGURE 5. Interferogram reconstruction for data far removed from the central peak.



$$\text{Instantaneous frequency} = \dot{\phi}(t) = \frac{\text{radial velocity of resultant}}{\text{radius of resultant}}$$

FIGURE 6. Phasor representation of the analytic form of the sum of two sine waves.

APPENDIX A

A SHORT DESCRIPTION OF THE INTERFEROGRAM SIGNAL

A Michelson interferometer was used to generate an interferogram signal which was then recorded on the Ampex SP 300 analog tape recorder. Also recorded was a clock waveform, a 2 kHz sine wave, which was used on playback to trigger an analog-to-digital converter for time series samples of the replayed interferogram waveform. For the purpose of the analysis it was assumed that the sample rate was one per second, not the actual two thousand samples per second. (Only the envelope and frequency computation technique was of interest here. The interferogram waveform was just a convenient source of data.) About 950 samples were taken of the one waveform used in this paper. Not all of them were used in the analysis. Figure A-1 illustrates the general characteristics of this waveform.

NOTE: SAMPLE RATE = 2×10^3 SAMPLES PER SECOND

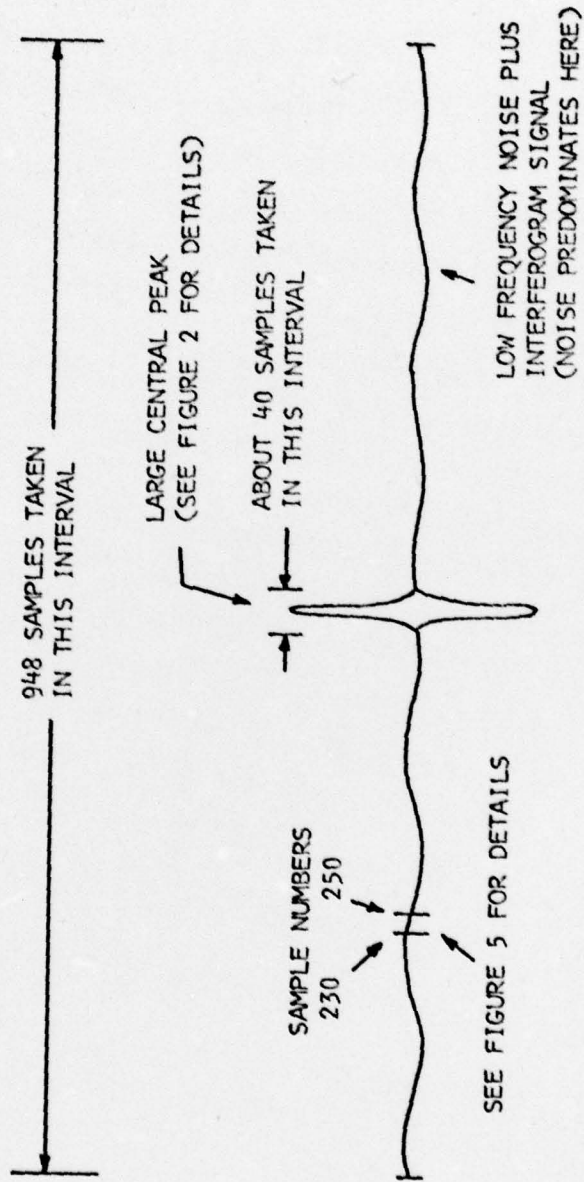


FIGURE A-1. ILLUSTRATION OF THE GENERAL CHARACTERISTICS OF THE INTERFEROGRAM WAVEFORM.
NOT TO SCALE.